THE JOURNAL OF BIOLOGICAL CHEMISTRY VOL. 282, NO. 34, pp. 24784–24791, August 24, 2007

Bacterial Expression, NMR, and Electrophysiology Analysis of Chimeric Short/Long-chain α-Neurotoxins Acting on Neuronal Nicotinic Receptors*

Received for publication, December 7, 2006, and in revised form, May 15, 2007 Published, JBC Papers in Press, June 18, 2007, DOI 10.1074/jbc.M611263200

Ekaterina N. Lyukmanova[‡], Zakhar O. Shenkarev[‡], Alexey A. Schulga[‡], Yaroslav S. Ermolyuk[‡], Dmitry Yu. Mordvintsev[‡], Yurii N. Utkin[‡], Mikhail A. Shoulepko[§], Ron C. Hogg[¶], Daniel Bertrand[¶], Dmitry A. Dolgikh[‡§1], Victor I. Tsetlin[‡], and Mikhail P. Kirpichnikov[‡§]

From the [‡]Shemyakin-Ovchinnikov Institute of Bioorganic Chemistry, Russian Academy of Sciences, 16/10 Miklukho-Maklaya Str., 117997 Moscow, Russia, [§]Moscow State University, 119899 Moscow, Russia, and [¶]Department of Neuroscience, Centre Medical Universitaire, Medical Faculty, 1 Rue Michel Servet, CH-1211 Geneva 4, Switzerland

Different snake venom neurotoxins block distinct subtypes of nicotinic acetylcholine receptors (nAChR). Short-chain α-neurotoxins preferentially inhibit muscle-type nAChRs, whereas long-chain α-neurotoxins block both muscle-type and α7 homooligomeric neuronal nAChRs. An additional disulfide in the central loop of α- and κ-neurotoxins is essential for their action on the α7 and α3β2 nAChRs, respectively. Design of novel toxins may help to better understand their subtype specificity. To address this problem, two chimeric toxins were produced by bacterial expression, a short-chain neurotoxin II *Naja oxiana* with the grafted disulfide-containing loop from long-chain neurotoxin I from *N. oxiana,* while a second chimera contained an additional A29K mutation, the most pronounced difference in the central loop tip between long-chain α-neurotoxins and κ-neurotoxins. The correct folding and structural stability for both chimeras were shown by ^{1}H and ^{1}H-^{15}N NMR spectroscopy. Electrophysiology experiments on the nAChRs expressed in *Xenopus* oocytes revealed that the first chimera and neurotoxin I block α7 nAChRs with similar potency (IC_{50} 6.1 and 34 nM, respectively). Therefore, the disulfide-confined loop endows neurotoxin II with full activity of long-chain α-neurotoxin and the C-terminal tail in neurotoxin I is not essential for binding. The A29K mutation of the chimera considerably diminished the affinity for α7 nAChR (IC_{50} 126 nM) but did not convey activity at α3β2 nAChRs. Docking of both chimeras to α7 and α3β2 nAChRs was possible, but complexes with the latter were not stable at molecular dynamics simulations. Apparently, some other residues and dimeric organization of κ-neurotoxins underlie their selectivity for α3β2 nAChRs.

Nicotinic acetylcholine receptors (nAChRs)[2] belong to the class of ligand-gated ion channels (1–3). All nAChRs are composed of five homologous subunits, which span the plasma membrane to form a transmembrane ion-conducting pore. The muscle-type receptors are composed of four types of subunits, $\alpha 2\beta\gamma\delta$ in the fetal and $\alpha 2\beta\epsilon\delta$ in the mature receptor. The best studied nAChR of this type is the receptor from electric organ of ray *Torpedo marmorata* (4). Neuronal receptors consist of two types of subunits, α (α2–α10) and β (β2–β4), and can have homooligomeric (for example, α7-type nAChR) or heterooligomeric (for example, α3β2-type receptor) composition. Neuronal nAChRs are widely expressed both pre- and postsynaptically, and presynaptic receptors modulate synaptic activity and the release of different neurotransmitters. Neuronal nAChRs are found also in non-neuronal tissues, such as keratinocytes and pulmonary and other tissues (5–8).

Because of their role in cellular communication, nAChRs play important roles in the normal functioning of the organism. Dysfunctions of these receptors have been proposed to contribute to a number of disorders of the central and peripheral nervous systems such as schizophrenia, epilepsy, depression, nicotine and alcohol dependence, Alzheimer disease, Parkinson disease, and autism (9–17). Distinct nAChR subtypes are involved in different disorders, and proper treatment of such diseases requires new therapeutic agents that are specific for a defined receptor subtype.

α-Neurotoxins from snake venoms are natural potent inhibitors of nAChRs. These toxins are small proteins with a "three-fingered" structure formed by three β-structural loops stabilized by disulfide bonds (18–20). α-Neurotoxins can be subdivided into several classes according to their biological and structural properties. Short-chain α-neurotoxins (4 disulfide bonds, 60–62 amino acid residues) selectively inhibit only muscle-type nAChRs, whereas long-chain α-neurotoxins (5 disulfide bonds, 66–75 amino acid residues) with an additional disulfide bond in the tip of the central loop can inhibit both muscle and neuronal α7 nAChRs (19, 20). There are κ-neurotoxins (5 disulfide bonds, 66 amino acid residues) that also contain an additional disulfide bond in the central loop and block neuronal α3β2 nAChR (21).

Site-directed mutagenesis (22, 23), chemical modification studies (24–26), and investigation of synthetic chimeric short/long-chain α-neurotoxins (27) indicate that the central loop fragment with fifth disulfide bond is essential for interaction of

* This work was supported by the Russian Academy of Sciences (program on molecular and cellular biology) and the Russian Foundation for Basic Research (Projects 05-04-48918, 05-04-48932). The costs of publication of this article were defrayed in part by the payment of page charges. This article must therefore be hereby marked "*advertisement*" in accordance with 18 U.S.C. Section 1734 solely to indicate this fact.

[1] To whom correspondence should be addressed. Tel.: 7-495-3368011; Fax: 7-495-3352888; E-mail: dolgikh@nmr.ru.

[2] The abbreviations used are: nAChR, nicotinic acetylcholine receptor; NTII, neurotoxin II from *N. oxiana*; NTI, neurotoxin I from *N. oxiana*; NTII/I, chimera of NTII and NTI; STII, *E. coli* heat-stable enterotoxin II; AChBP, acetylcholine-binding protein; HPLC, high pressure liquid chromatography.

α- and κ-neurotoxins with neuronal α7 and α3β2 receptors, respectively. Recently the structural basis of interaction between the central loop of a toxin and nAChR was revealed by x-ray investigation of a crystallized complex of long-chain α-cobratoxin from *Naja kaouthia* with the acetylcholine-binding protein from *Lymnaea stagnalis* (AChBP) (28). (AChBP is a natural water-soluble homopentameric protein that is an excellent model of the ligand-binding domain of the nAChR) (29, 30). Direct intermolecular contacts between the fifth disulfide of the neurotoxin, Cys-27-Cys-31 (numbers are given for neurotoxin I), and the residues on the surface of the adjacent subunit of the AChBP were observed in this complex.

The structure of α-cobratoxin-AChBP complex explains common principles of interaction between α-neurotoxins and nAChRs. However, the exact structural features that determine the selectivity between different nAChR subtypes remain unclear. Design of chimeric molecules bearing features of toxins from different groups can shed light on this problem.

In the present communication we describe heterologous expression in *Escherichia coli* of chimeric short/long-chain α-neurotoxins. We demonstrate using electrophysiology on human α7 nAChR expressed in *Xenopus* oocytes that grafting the disulfide-confined tip of the neurotoxin I *N. oxiana* on a short-chain neurotoxin II from the same venom makes the latter as active as neurotoxin I itself. An additional mutation, A29K, has been done in this chimera to test the hypothesis of Bourne *et al.* (28) that the Lys-29 is the major factor underlying the difference in specificity between the long-chain α-neurotoxins and κ-neurotoxins toward α7 and α3β2 nAChRs, respectively. This mutation considerably decreased the activity against α7 nAChRs but showed no inhibition of human α3β2 nAChRs.

EXPERIMENTAL PROCEDURES

Comparison of NTII Spatial Structure with Structures of Long-chain α-Neurotoxins—The atomic coordinates for NTII and five long-chain neurotoxins (neurotoxin I, α-bungarotoxin, α-cobratoxin, toxin B, κ-bungarotoxin) were taken from the Protein Data Bank (PDB codes 1NOR, 1NTN, 2ABX, 1CTX, 1TXA, 1KBA, respectively). Superimposition of structures and root mean square deviation calculation was done in MolMol program (31).

Expression of NTII Gene in E. coli—A synthetic NTII gene (32) was joined to a sequence encoding the signal peptide of *E. coli* heat-stable enterotoxin II (STII) (NCBI accession number M35729). This fusion gene was placed under the control of the T7 promoter in an expression vector pET-22b (Novagen) between the NdeI and HindIII sites. The resultant plasmid was named pET22b/STII/NTII.

Engineering of the Mutant Neurotoxins—The fragment of the NTI central loop was introduced into the NTII molecule using the QuikChange™ site-directed mutagenesis kit (Stratagene) on the basis of pET22b/STII/NTII. Primer 5′-CTACAAAAAG-TGGTGGTGCGACGCGTGGTGCGGTTCCCGTGGTACC-ATCATC-3′, coding the disulfide-containing fragment of central loop of NTI, was used as direct primer. Primer 5′-GATGATG-GTACCACGGGAACCGCACCACTTGTCGCACCACCAC-TTTTTGTAG-3, partly complementary to the direct primer sequence, coding the disulfide-containing fragment of the central loop of NTI with substitution Ala/Lys, was used as reverse primer. Amplification was performed on the Mastercycler® Personal PCR amplifier (Eppendorf, Germany).

Bacterial Expression, Isolation, and Purification of Recombinant Neurotoxins—BL21(DE3) *E. coli* cells were transformed with the recombinant vectors and plated onto Petri dishes with Luria Bertani agar containing ampicillin (100 μg/ml). Several colonies were then inoculated with minimal mineral M9 medium (0.4% glycerol, 3 g/liter KH_2PO_4, 6 g/liter Na_2HPO_4, 0.5 g/liter NaCl, 0.24 g/liter $MgSO_4$, 0.01 g/liter $CaCl_2$, 2 g/liter NH_4Cl, 1% thiamine chloride, 0.2% yeast extract) containing ampicillin (100 μg/ml). The cells were cultivated at 37 °C and moderate mixing (250 rpm) until optical density of the bacterial culture had reached 0.6 optical units at 600 nm wavelength. After that, gene expression was induced by adding isopropyl-1-thio-β-D-galactopyranoside to a final concentration of 0.05 mM. After 15 h of cultivation the cell culture was centrifuged (14,000 × *g*, 30 min, 4 °C). Growth medium was acidified to pH 4.5, heated at 70 °C during 30 min, and centrifuged once more (14000 × *g*, 30 min, 4 °C). The supernatant was diluted 2-fold with Milli-Q deionized water (Millipore). The first step of purification was made using cation exchange SP-Sepharose Fast Flow resin (GE Healthcare), equilibrated in 10 mM CH_3COONa, pH 5.0. Protein fractions were eluted in the linear gradient of NaCl (from 0 mM to 1 M), and fractions containing modified neurotoxins were collected at 0.25 mM NaCl. The mutant toxins were additionally purified on a MonoS HR5/5 column (GE Healthcare), equilibrated with 10 mM CH_3COONa, pH 5.0, and eluted from the column with 0.4 M NaCl. The buffer of protein samples was changed to 0.2 M CH_3COOH using Sephadex™ G-25 NAP™-5 and NAP™-10 columns (GE Healthcare). Finally, protein solutions were lyophilized overnight on an Alpha I-5 freeze dryer (Martin Christ Gefriertrocknungsanlagen GmbH). Protocol for production and purification of ^{15}N-labeled NTII and NTII/I chimera was the same as in the case of non-labeled toxins, with the exception of using $^{15}NHCl$ as a sole source of nitrogen ($^{15}N > 99\%$; Martek Biosciences).

Analysis of Recombinant Toxins—All the steps of protein production, isolation, and purification were controlled by 12% Tris/Tricine-SDS-PAGE (33). The N-terminal amino acid sequence of the obtained proteins was determined on the Applied Biosystems 470A gas-phase sequenator. Recombinant neurotoxins were analyzed by mass spectrometry using a matrix-assisted laser desorption ionization Daltonics Ultraflex II TOF/TOF (time-of-flight) instrument (Bruker) equipped with nitrogen laser and time-of-flight mass analyzer. All NMR experiments were performed on a 500-MHz DRX-500 spectrometer (Bruker). One-dimensional ^1H and two-dimensional ^1H-^{15}N HSQC spectra were measured for 1 mM protein solutions in H_2O (10% D_2O).

Electrophysiology—Expression and electrophysiological recording from nAChRs was carried out as described previously (34). Briefly, oocytes were injected intranuclearly with 2 ng of cDNA that coded for either the human α7 or α3β2 receptors (cDNAs were a gift from J. P. Changeux). All recordings were performed in OR2 medium that contained 82.5 mM NaCl, 2.5 mM KCl, 5 mM HEPES, 2.5 mM $CaCl_2$, 1 mM MgCl adjusted to pH 7.4 with

NaOH. Acetylcholine and toxins were dissolved in the OR2 medium just prior to use. Recordings were carried out at −100 mV. Oocyte loading, penetration, and voltage clamping were carried out by an automated system based around a liquid-handling robot controlled by in-house software. Solution exchanges were automated and carried out by the same liquid handler. Control responses were recorded before toxin exposure and toxin incubation was carried out in the recording chamber during 3 min using a static bath technique. Peak current amplitude was plotted as a function of the toxin concentration on a semilog scale. Dose-response curves for toxin inhibition were fit with the equation $y = 1/1\ ([\text{toxin}]/(IC_{50})^n)$, where y is the normalized response, [toxin] is the toxin concentration, and n is the Hill coefficient. ACh concentration was close to the EC_{50} for receptor activation, and toxin incubation time was determined by testing receptor responses after increasing toxin incubation times. Equilibrium was assumed to be reached when no further inhibition of the response was seen.

Modeling of Chimeras and Their nAChR Complexes—The models of the chimeric toxins were built using homology modeling technique under MODELLER with further molecular dynamics refinement in CHARMM'27 and stochastic dynamics under GROMACS. Further relaxation was done with Minimization routine in CHARMM'27 force field under TINKER program. 3-ns trajectories were calculated at the temperature 300 K and dielectric permittivity $e = 1$.

The models of the nAChR subunits and their assemblies were built similarly as described in Ref. 35 for *Torpedo californica* nAChR subunits; the structure of the α-cobratoxin complex with AChBP (PDB code 1YI5) was additionally used as a template. Visual analysis was carried out with SPDBViewer version 3.7 sp5 program.

Docking simulations were performed with both AutoDock 3.05 and HEX 4.5 programs. The solutions of the complexes were relaxed and underwent molecular dynamics simulation with GROMACS for 100–200-ps trajectories.

RESULTS

Construction of Short/Long-chain α-Neurotoxin Chimeras—The chimeric toxins were built on the scaffold of the short-chain NTII chosen for several reasons. First, NTII has low activity against neuronal nAChRs ($IC_{50} > 1\ \mu M$), thus providing reliable reference for detection of even subtle changes in affinity. Second, high level bacterial expression systems for this toxin had previously been developed (32, 36) and could be adapted for production of chimeras.

To find the most appropriate donor for the disulfide-confined fragment of the central loop, we compared, in terms of atomic pair-wise root mean square deviation, the spatial structures of several long-chain neurotoxins (neurotoxin I, α-bungarotoxin, α-cobratoxin, toxin B, κ-bungarotoxin) with the three-dimensional structure of NTII. The molecules were superimposed by fitting atomic coordinates for Cα atoms from four conserved disulfides and from two β-strands that form the central loop (residues 3, 14, 21–26, 37–42, 46, 57, 58, 63, numbers are given for NTI). The minimal value of pair-wise root mean square deviation with NTII for this group of atoms (0.89 Å) was found for NTI from *N. oxiana* (NTI), and this long-chain α-neurotoxin was chosen as donor, ensuring less structural perturbation during "transplantation." To this end, Ser-29, Asp-30, and His-31 of NTII were replaced by Cys-27, Asp-28, Ala-29, Trp-30, Cys-31, Gly-32, and Ser-33 of NTI (Fig. 1).

Bacterial Expression, Isolation, and Purification of Recombinant Toxins—Recombinant neurotoxins were produced in *E. coli* BL21(DE3) strain under the transcriptional control of a T7 promoter. After induction with isopropyl-1-thio-β-D-galactopyranoside, toxins began to accumulate in periplasm and growth medium and were processed accurately during the secretion process. Chimeras were isolated from growth medium in two steps by separation on cation exchange SP-Sepharose Fast Flow resin and MonoS HR5/5 column (GE Healthcare). The toxin purity was checked by reversed phase HPLC (Fig. 2). It is seen that the elution times for chimeric toxins are between those for NTII and NTI. The substitution of alanine residue by lysine in NTII/I[A29K] resulted in decreased hydrophobicity manifested in shorter retention time on reversed phase HPLC.

The final yield of the mutant toxins containing five disulfide bonds was ~1 mg/liter of bacterial culture in the case of NTII/I chimera and 5 mg for NTII/I[A29K], which is several times lower than yield of NTII (~20 mg/l) in this system. The yields of ^{15}N-labeled NTII and NTII/I chimera were similar to the yields of non-labeled proteins. The lower yields of chimeric toxins can be explained by the presence of an additional disulfide bond. Nevertheless, the obtained quantities of chimeras were sufficient for structural and electrophysiological investigations.

The N-terminal analysis using Edman's degradation showed that the obtained recombinant toxins had N-terminal sequences identical to that of the wild-type NTII. Thus, mutant neurotoxins were secreted into periplasm and the signal peptide STII was properly cleaved. Mass spectral analysis of natural NTII and mutant neurotoxins revealed very good correlation between the determined masses and expected calculated values (8020 Da *versus* 8021, 6878 *versus* 6877, 7257 *versus* 7258, and 7314 *versus* 7315 for NTI, NTII, NTII/I and NTII/I[A29K], respectively).

Structural Analysis of Recombinant Chimeras—The fragments grafted to NTII consist of 7 residues and include additional disulfide bond. Introduction of these fragments might affect the stability and spatial structure of chimeric toxins. We used NMR spectroscopy to estimate possible changes in spatial structure of chimeras.

The one-dimensional ^1H NMR spectra for recombinant NTII/I and NTII/I[A29K] displayed narrow NMR lines and a large dispersion of signals in amide and aliphatic regions. Comparison with the one-dimensional ^1H spectrum of NTII revealed almost coinciding envelope for all three one-dimensional spectra, with intact position of several characteristic non-overlapping resonances and with additional signals in the case of chimeras (data not shown). The ^1H-^{15}N HSQC spectra for recombinant ^{15}N-labeled NTII and NTII/I (Fig. 3, *A* and *B*) revealed almost complete correspondence of ^1H and ^{15}N resonance frequencies for common residues in both toxins. The detailed analysis of these spectra allowed us to make resonance assignment for the NTII/I chimera. Comparison of the one-dimensional ^1H spectrum of NTII/I[A29K] with the HSQC

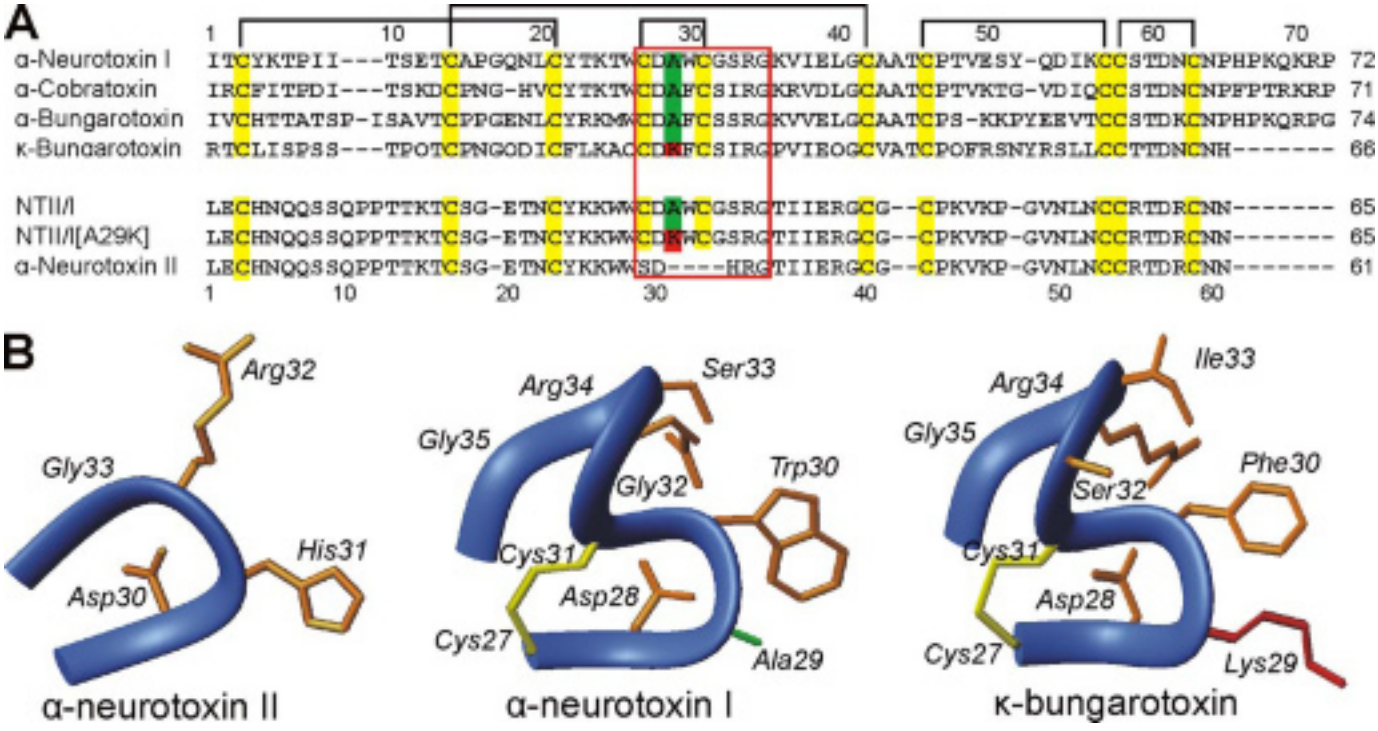

FIGURE 1. **Comparison of neurotoxin structures.** *A*, alignment of amino acid sequences of snake neurotoxins and chimeric toxins (residue numbers are given for NTI and NTII). Residues belonging to the tip of the central loop are enclosed in the *red rectangle*, cysteines are highlighted by the *yellow background*, Lys(Ala) in position 29 are highlighted by the *red(green)* background. *B*, spatial structures of the central loop fragments for NTII, NTI, and κ-bungarotoxin. Color codes for Cys-27 to Cys-31, Ala-29, and Lys-29 are the same as in *panel A*.

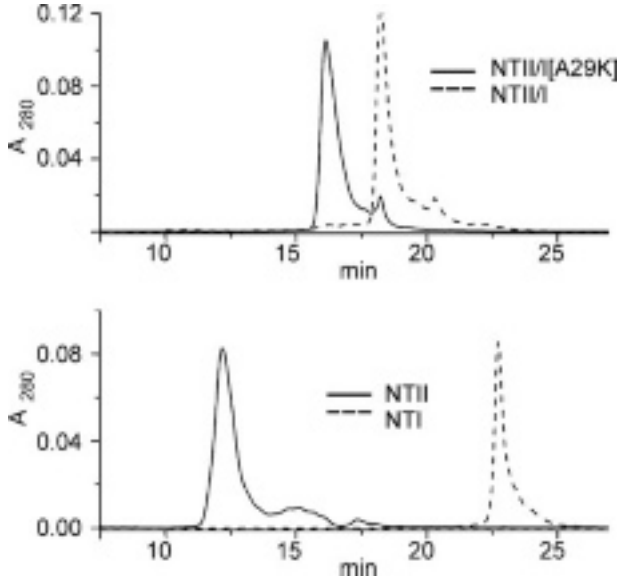

FIGURE 2. **HPLC analysis of recombinant neurotoxins.** The chromatography was performed on a Jupiter C18 column (4.6 × 250 mm) using a gradient of acetonitrile in water (0.1% trifluoroacetic acid) from 15 to 45% in 30 min at a flow rate of 1 ml/min.

spectrum of NTII/I (Fig. 3*C*) indicated that point mutation A29K does not change the spatial structure of chimeric toxin. Thus, recombinant chimeras share a common, relatively rigid spatial structure with neurotoxin II. This conclusion was also supported by CD spectroscopy data (not shown).

Electrophysiological Analysis of Chimeras—The biological activity of modified neurotoxins was tested *in vitro* by measuring the ability to inhibit acetylcholine-induced currents at neuronal α7 and α3β2 nAChRs expressed in *Xenopus laevis* oocytes. The capacity of neurotoxins NTI and NTII to inhibit ACh-evoked currents at the human α7 nAChR was first examined. Fig. 4*A* shows that NTI blocked the human α7 nAChR with an IC_{50} of 34 nM, whereas the short-chain NTII had no effect. Then the effects of the NTII/I and NTII/I[A29K] chimeras at the human α7 nAChR were assessed. The inclusion of the central loop tip containing the additional disulfide in NTII conveyed activity at α7 nAChRs to NTII/I chimera (IC_{50} of 6.1 nM) (Fig. 4*B*). The second chimera, NTII/I[A29K], also inhibited ACh-evoked currents; however, the A29K substitution in the tip considerably decreased the activity at the α7 nAChR (IC_{50} 126 nM, Fig. 4*C*). Neither the native toxins NTI and NTII nor the chimeras NTII/I and NTII/I[A29K] inhibited currents at human α3β2 nAChRs at concentrations up to 1 μM (data not shown).

Modeling of Spatial Structures for Chimeric Toxins and Their Complexes with nAChRs—The spatial structures of the chimeric toxins were constructed using homology modeling on the basis of three-dimensional structures of NTI, NTII, and α-cobratoxin. The introduction of the insert from the long-chain neurotoxin and subsequent A29K replacement did not affect the stability of the general fold of the molecule and did not influence the flexibility of the disulfide-fixed core taken from NTII.

Constructed models of the nAChR subunits and their assemblies (α7 and α3β2) were similar to those built previously (35, 37). The control docking of NTII and NTI to α7 and α3β2 nAChRs gave stable complex only in the case of NTI/-α7 (similar to 1YI5) (28). Docking of NTII/I chimera was possible both

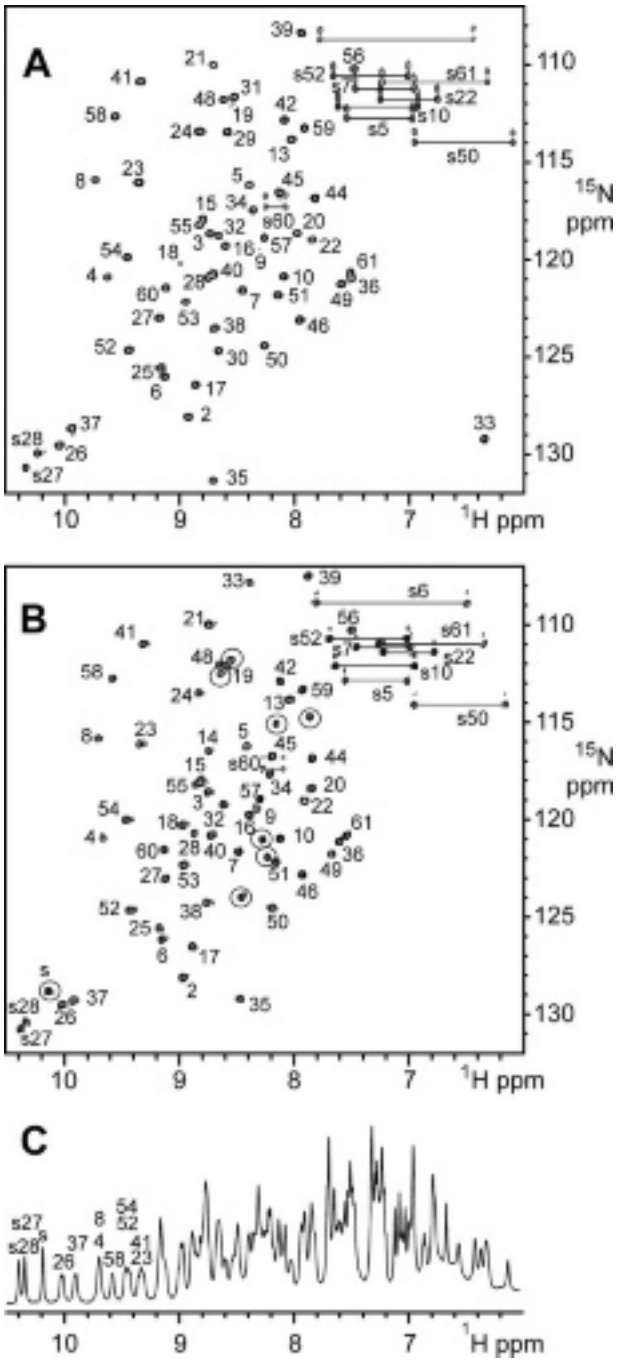

FIGURE 3. **NMR analysis of recombinant NTII and chimeric toxins.** *A*, ^{1}H-^{15}N HSQC NMR spectra of NTII, pH 5.9, 30 °C. Cross-peaks of NH groups are labeled by residue numbers, assignments are taken from Bocharov *et al.* (36), cross-peaks of side chains of Trp, Asn, and Gln are labeled with "s." The cross-peaks of NH Gly-33 are folded in ^{15}N dimension. Residue numbers are given for NTII. *B*, ^{1}H-^{15}N HSQC NMR spectra of NTII/I, pH 5.7, 30 °C. Assignment was made by analogy with *panel A*, coinciding cross-peaks are numbered with NTII numbers. Cross-peaks for 7 grafted residues are *encircled*. *C*, amide and aromatic regions of ^{1}H NMR spectra of NTII/I[A29K], pH 5.7, 30 °C. Assignment for several downfield signals is shown.

to α7 and α3β2, but only NTII/I-α7 complex was stable during subsequent molecular dynamics simulation. The main interactions were with the C-loop of the nAChR principal site, similar to α-cobratoxin complex (28). However, the position of the whole chimera molecule resembled NTII bound to the α/γ interface of Torpedo nAChR (35).

Docking studies suggest that the A29K substitution in the NTII/I[A29K] chimera should not influence the position of the chimeric toxin on the receptor interface. However, the affinity of NTII/I[A29K] chimera to the α7 nAChR subtype was higher than to α3β2 nAChR (estimated energies of interaction are 1400 KJ/mol/binding site and 340 KJ/mol/binding site, respectively). Moreover, the chimera complex with α3β2 nAChR was unstable under MD simulation.

DISCUSSION

Until recently, information on the mode of interaction of diverse snake toxins with various nAChRs was based mainly on mutations of toxins and/or receptors, pair-wise mutagenesis, and cross-linking (20). Such approaches revealed, for example, some differences between short-chain and long-chain α-neurotoxins in the involvement of their three loops in the interaction with muscle-type nAChRs (38–41). It was also shown that a number of residues of the muscle-type receptors participate in the interaction with the toxins of both groups, whereas some residues are important for binding with only short-chain neurotoxins and others with long-chain neurotoxins (42).

Determination of the crystal structure for the acetylcholine-binding proteins (AChBPs) (29, 43), their complexes with different agonists (44), and antagonists such as α-cobratoxin and α-conotoxins (28, 37, 45, 46) has provided a basis for detailed analysis of the nAChR interaction with snake neurotoxins. This model can help to better understand the topography of their binding surfaces and choose new mutations that in principle can give novel toxins of higher affinity and better selectivity for a particular nAChR subtype.

As mentioned in the Introduction, the action of snake toxins on neuronal α7 or α3β2 nAChRs requires the presence of an intact disulfide bond in the central loop of the toxin molecule (22–26). The x-ray analysis of the α-cobratoxin complex with *L. stagnalis* AChBP revealed direct contacts between this disulfide bond and residues in the binding site (28). This analysis also detected contacts of 10 α-cobratoxin residues whose involvement in binding to α7 nAChRs has been previously suggested from mutagenesis studies (22, 23, 25). Although the AChBP is considered a model for all types of nAChRs, the available data do not answer the question why, for example, long-chain α-neurotoxins have a high affinity for α7 nAChRs whereas κ-neurotoxins target α3β2 nAChRs. Because the disulfide-confined tip of the central loop is a prerequisite for binding to both these nAChRs, one could assume that the differences in specificity might stem from the amino acid differences in this fragment. (It should be kept in mind that κ-neurotoxins exist as dimers, which could also affect their nAChR selectivity (47, 48). The most obvious difference is the presence of Lys-29 in κ-neurotoxins whereas the homologous position in α-neurotoxins is occupied by Ala-29 (Fig. 1). Bourne *et al.* (28) suggested that this substitution may be one of the major factors determining specificity to a particular nAChR subtype. To test this hypothesis, we designed the chimera with A29K substitution.

Mutagenesis (22, 23), NMR, and x-ray structures of long-chain α-neurotoxin complexes with nAChR fragments or combinatorial peptides (49–52), as well as the crystal structure for the AChBP complex with α-cobratoxin (28), showed that some

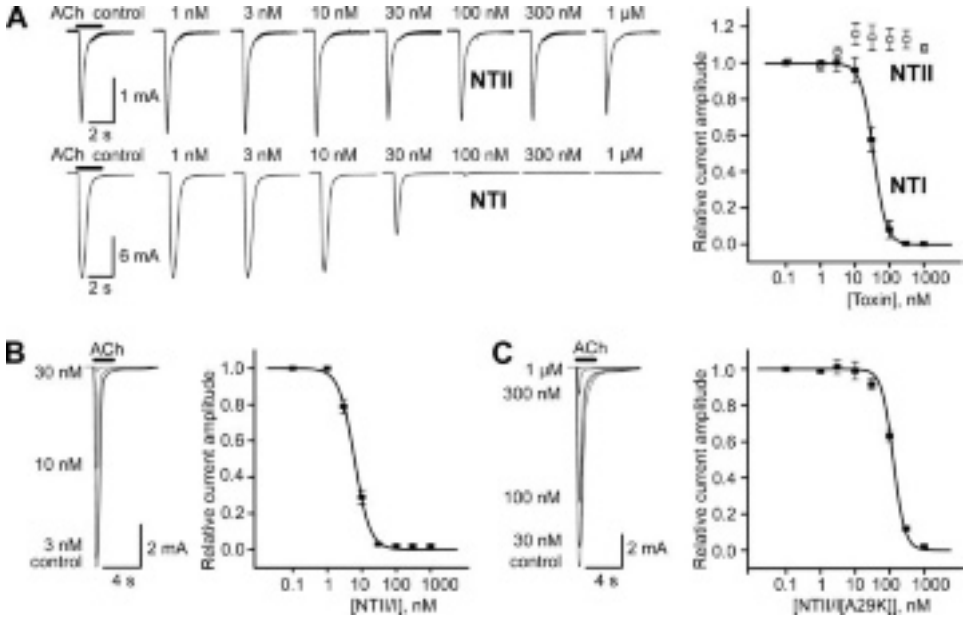

FIGURE 4. **Effect of wild-type NTI, NTII, and recombinant chimeras on ACh-activated currents at human α7 nAChRs.** *A*, long-chain toxin NTI inhibits ACh-activated currents at α7 nAChRs in a concentration-dependent manner (IC_{50} 34 nM, n_H 2.3), whereas the short-chain toxin NTII has no effect at concentrations up to 1 μM. Currents were activated with 200 μM Ach. The control current in the absence of toxin is shown on the *left* and following preincubation with 1, 3, 10, 30, 100, and 300 nM and 1 μM toxin. *B*, chimera NTII/I inhibits ACh-activated currents at α7 nAChRs with an IC_{50} of 6 nM and n_H 1.9. *C*, chimera NTII/I[A29K] inhibits ACh-activated currents at α7 nAChRs with an IC_{50} of 126 nM and n_H 2.6.

residues of the α-neurotoxin C-terminal tail may participate in binding with the α7 nAChR. Because the C-terminal tail is absent in κ-neurotoxins acting on α3β2 nAChRs (Fig. 1) and in short-chain α-neurotoxins, we used short-chain neurotoxin II *N. oxiana* as a scaffold for chimeras. Chimeras were constructed on the basis of this toxin by inserting a disulfide-confined fragment from the central loop of long-chain α-neurotoxin, namely neurotoxin I *N. oxiana.* Analysis of the three-dimensional structures of NTII and a number of long-chain α-neurotoxins indicated that the introduction of the loop fragment from neurotoxin I might lead only to small perturbations of the NTII central loop conformation. Indeed, NMR and modeling data confirmed these expectations. Because NTII itself practically does not interact with neuronal nAChRs ($IC_{50} > 1$ μM), the chimeras allowed evaluation of the role of the introduced fragment in the interactions with α7 and α3β2 nAChRs.

Chimeras were produced by bacterial expression, which was quite successful in the case of NTII and its ^{15}N-^{13}C-labeled analogue (36). Introduction of the fifth disulfide into the neurotoxin molecule resulted in a lower yield of the target protein. However, the conditions were found that gave sufficient amounts of the products and allowed us to obtain one of the chimeras (NTII/I) in ^{15}N-labeled form for detailed structural study (Fig. 3).

The electrophysiology experiments on α7 nAChRs expressed in *X. laevis* oocytes revealed that the chimera NTII/I had a comparable activity (IC_{50} = 6.1 nM) to the naturally occurring neurotoxin I (IC_{50} = 34 nM). This finding indicates that the C-terminal tail of NTI is not essential for binding to α7 nAChR.

It should be noted that Mourier *et al.* (27), who were the first to make a chimera of long- and short-chain α-neurotoxins, with the aid of peptide synthesis prepared α-toxin *Naja nigricollis* containing the central loop tip from α-bungarotoxin. This chimera bound to α7 nAChR, with K_d 100 nM, being 100-fold less active than native α-bungarotoxin.

The A29K substitution in the tip of the chimera NTII/I[A29K] markedly decreased the activity at α7 nAChR. However, neither NTI itself nor the chimeras showed activity toward α3β2 nAChRs. Thus, our results indicate that introduction of a positive charge (Lys-29) to the disulfide-confined tip of the central loop does not shift the specificity of α-neurotoxin from the α7 to α3β2 nAChRs.

Our results are in agreement with the available literature data showing that the interaction of snake venom neurotoxins with nAChRs depends on numerous points of contacts. The overall toxin affinity for the receptor is most likely the sum of several contributions, some from the residues of the central loop, others may include the N-terminal loop or C terminus. The involvement of the N-terminal loop and the C terminus in binding appears to vary among different α-neurotoxins (23, 53). Although a single mutation of α-neurotoxins can cause pronounced changes in the affinity for a given receptor subtype, no shifts in the nAChR subtype specificity were registered.

In this respect α-neurotoxins differ from α-conotoxins, small subtype-selective nAChR antagonists from cone snails. For these peptides, single amino acid substitutions may be sufficient not only to enhance the affinity at a particular nAChR but also to change the specificity. For example, the A10L substitution in α-conotoxin PnIA induced a shift in the specificity from α3β2 to α7 nAChR (54). An additional substitution (D14K) in PnIA gave a "double mutant" with a slightly increased affinity for α7 nAChR and a 10-fold enhancement of affinity for *L. stagnalis* AChBP. The crystal structure of this double mutant complex with AChBP provided an explanation why the affinity was increased toward *L. stagnalis* AChBP, but not to *Aplysia californica* AChBP (37). Interestingly, in complexes with AChBP (37, 45, 46) α-conotoxins occupy approximately the same site as the tip of the central loop of α-cobratoxin (28).

Simulation of binding of both chimeras to α7 nAChR revealed that the Lys-29 residue could not make any specific interaction with the α7 nAChR residues and was exposed to the solvent, being repulsed by Lys-192-positive charge (numbering by human α7 nAChR), see Fig. 5. On the contrary, Ala-29 had weak hydrophobic contacts with the main chain C-loop residues. This distinction could explain the decreased affinity of NTII/I[A29K] to α7 nAChR. On the other hand, modeling suggests that Lys-29 of NTII/I[A29K] can make a contact with Glu-190 of α3 subunit in the α3β2 nAChR. Despite that, the

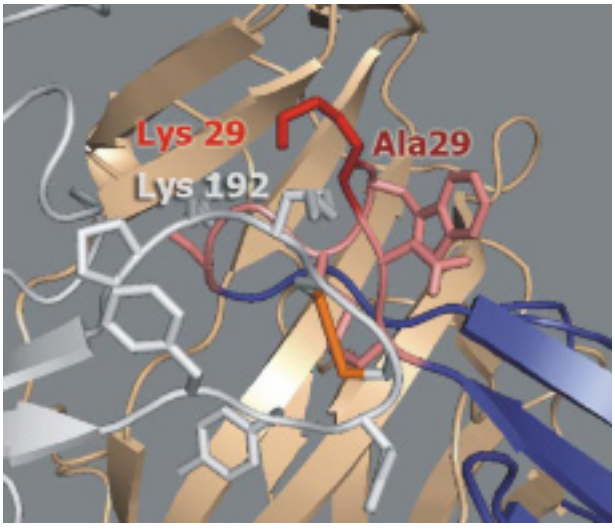

FIGURE 5. **Model of the chimeric toxin bound to α7 nAChR (zoom at the inserted NTI fragment).** The NTII part of the toxin is in *blue*, NTI is in *pink*. One subunit of nAChR (principal side of the interface) is in *white*; the other (complementary side) is in *wheat*. Side chains of the residues of the inserted NTI portion and of the C-loop of the principal side are shown. The Ala-29 of the toxin is in *brick*; the corresponding position of the Lys-29 is marked in *red*.

complex NTII/I[A29K]-α3β2 was unstable during MD simulation. It seems that some other interactions, including those due to a dimeric structure, are the basis of the known specificity of κ-neurotoxins to the α3β2 nAChR.

In summary, bacterial expression gave us chimeras combining structural features of short- and long-chain snake venom neurotoxins. Their individuality and chemical structure were confirmed by analytical HPLC and mass spectrometry, and spatial structure was characterized by NMR and computer modeling. Electrophysiology experiments showed that incorporation of a disulfide-confined tip makes a short-chain neurotoxin fully active against α7 nAChR. Modeling of the chimera complexes with α7 and α3β2 nAChRs in general agrees with the electrophysiology data, but deeper understanding of toxin specificity toward a particular nAChR subtype will require a larger series of mutants and refined computational approaches.

Acknowledgments—We thank Prof. Alexander Arseniev, Dr. Innokenty Maslennikov, and Dr. Kirill Pluzhnikov for fruitful discussions and Dr. Eduard Bocharov for providing the spectral assignment for ^{15}N-labeled NTII.

REFERENCES

1. Hucho, F., and Weise, C. (2001) *Angew. Chem. Int. Ed.* **40,** 3100–3116
2. Lindstrom, J. M. (2003) *Ann. N. Y. Acad. Sci.* **998,** 41–52
3. Karlin, A. (2002) *Nat. Rev. Neurosci.* **3,** 102–114
4. Unwin, N. (2005) *J. Mol. Biol.* **346,** 967–989
5. Li, X. W., and Wang, H. (2006) *Life Sci.* **78,** 1863–1870
6. Wang, H., Yu, M., Ochani, M., Amella, C. A., Tanovic, M., Susarla, S., Li, J. H., Wang, H., Yang, H., Ulloa, L., Al Abed, Y., Czura, C. J., and Tracey, K. J. (2003) *Nature* **421,** 384–388
7. Wang, Y., Pereira, E. F., Maus, A. D., Ostlie, N. S., Navaneetham, D., Lei, S., Albuquerque, E. X., and Conti-Fine, B. M. (2001) *Mol. Pharmacol.* **60,** 1201–1209
8. Plummer, H. K., III, Dhar, M., and Schuller, H. M. (2005) *Respir. Res.* **6,** 29
9. Bertrand, D. (2002) *Epilepsy Curr.* **2,** 191–193
10. Dohrman, D. P., and Reiter, C. K. (2003) *Brain Res.* **975,** 90–98
11. Tapper, A. R., McKinney, S. L., Nashmi, R., Schwarz, J., Deshpande, P., Labarca, C., Whiteaker, P., Marks, M. J., Collins, A. C., and Lester, H. A. (2004) *Science* **306,** 1029–1032
12. Hogg, R. C., and Bertrand, D. (2004) *Bioorg. Med. Chem. Lett.* **14,** 1859–1861
13. Martin-Ruiz, C., Lawrence, S., Piggott, M., Kuryatov, A., Lindstrom, J., Gotti, C., Cookson, M. R., Perry, R. H., Jaros, E., Perry, E. K., and Court, J. A. (2002) *Neurosci. Lett.* **335,** 134–138
14. Martin-Ruiz, C. M., Court, J. A., Molnar, E., Lee, M., Gotti, C., Mamalaki, A., Tsouloufis, T., Tzartos, S., Ballard, C., Perry, R. H., and Perry, E. K. (1999) *J. Neurochem.* **73,** 1635–1640
15. Martin-Ruiz, C. M., Haroutunian, V. H., Long, P., Young, A. H., Davis, K. L., Perry, E. K., and Court, J. A. (2003) *Biol. Psychiatry* **54,** 1222–1233
16. Martin-Ruiz, C. M., Lee, M., Perry, R. H., Baumann, M., Court, J. A., and Perry, E. K. (2004) *Brain Res. Mol. Brain Res.* **123,** 81–90
17. Shen, X. M., Ohno, K., Tsujino, A., Brengman, J. M., Gingold, M., Sine, S. M., and Engel, A. G. (2003) *J. Clin. Investig.* **111,** 497–505
18. Menez, A. (1998) *Toxicon* **36,** 1557–1572
19. Tsetlin, V. (1999) *Eur. J. Biochem.* **264,** 281–286
20. Tsetlin, V. I., and Hucho, F. (2004) *FEBS Lett.* **557,** 9–13
21. Grant, G. A., Frazier, M. W., and Chiappinelli, V. A. (1988) *Biochemistry* **27,** 3794–3798
22. Antil-Delbeke, S., Gaillard, C., Tamiya, T., Corringer, P. J., Changeux, J. P., Servent, D., and Menez, A. (2000) *J. Biol. Chem.* **275,** 29594–29601
23. Servent, D., Antil-Delbeke, S., Gaillard, C., Corringer, P. J., Changeux, J. P., and Menez, A. (2000) *Eur. J. Pharmacol.* **393,** 197–204
24. Grant, G. A., Luetje, C. W., Summers, R., and Xu, X. L. (1998) *Biochemistry* **37,** 12166–12171
25. Servent, D., Winckler-Dietrich, V., Hu, H. Y., Kessler, P., Drevet, P., Bertrand, D., and Menez, A. (1997) *J. Biol. Chem.* **272,** 24279–24286
26. Servent, D., Mourier, G., Antil, S., and Menez, A. (1998) *Toxicol. Lett.* **102–103,** 199–203
27. Mourier, G., Servent, D., Zinn-Justin, S., and Menez, A. (2000) *Protein Eng.* **13,** 217–225
28. Bourne, Y., Talley, T. T., Hansen, S. B., Taylor, P., and Marchot, P. (2005) *EMBO J.* **24,** 1512–1522
29. Brejc, K., van Dijk, W. J., Klaassen, R. V., Schuurmans, M., van Der, O. J., Smit, A. B., and Sixma, T. K. (2001) *Nature* **411,** 269–276
30. Sixma, T. K., and Smit, A. B. (2003) *Annu. Rev. Biophys. Biomol. Struct.* **32,** 311–334
31. Koradi, R., Billeter, M., and Wuthrich, K. (1996) *J. Mol. Graph.* **14,** 51–55
32. Liukmanova, E. N., Shul'ga, A. A., Aren'eva, D. A., Pluzhnikov, K. A., Dolgikh, D. A., Arsen'ev, A. S., and Kirpichnikov, M. P. (2004) *Bioorg. Khim.* **30,** 30–40
33. Schagger, H., and von Jagow, G. (1987) *Anal. Biochem.* **166,** 368–379
34. Hogg, R. C., Hopping, G., Alewood, P. F., Adams, D. J., and Bertrand, D. (2003) *J. Biol. Chem.* **278,** 26908–26914
35. Mordvintsev, D. Y., Polyak, Y. L., Levtsova, O. V., Tourleigh, Y. V., Kasheverov, I. E., Shaitan, K. V., Utkin, Y. N., and Tsetlin, V. I. (2005) *Comput. Biol. Chem.* **29,** 398–411
36. Bocharov, E. V., Lyukmanova, E. N., Ermolyuk, Y. S., Schulga, A. A., Pluzhnikov, K. A., Dolgikh, D. A., Kirpichnikov, M. P., and Arseniev, A. S. (2003) *Appl. Magn. Reson.* **24,** 247–254
37. Celie, P. H., Kasheverov, I. E., Mordvintsev, D. Y., Hogg, R. C., van Nierop, P., van Elk, R., Rossum-Fikkert, S. E., Zhmak, M. N., Bertrand, D., Tsetlin, V., Sixma, T. K., and Smit, A. B. (2005) *Nat. Struct. Mol. Biol.* **12,** 582–588
38. Antil, S., Servent, D., and Menez, A. (1999) *J. Biol. Chem.* **274,** 34851–34858
39. Teixeira-Clerc, F., Menez, A., and Kessler, P. (2002) *J. Biol. Chem.* **277,** 25741–25747
40. Fruchart-Gaillard, C., Gilquin, B., Antil-Delbeke, S., Le Novere, N., Tamiya, T., Corringer, P. J., Changeux, J. P., Menez, A., and Servent, D. (2002) *Proc. Natl. Acad. Sci. U. S. A.* **99,** 3216–3221
41. Ackermann, E. J., Ang, E. T., Kanter, J. R., Tsigelny, I., and Taylor, P. (1998) *J. Biol. Chem.* **273,** 10958–10964
42. Spura, A., Riel, R. U., Freedman, N. D., Agrawal, S., Seto, C., and Hawrot, E. (2000) *J. Biol. Chem.* **275,** 22452–22460

43. Celie, P. H., Klaassen, R. V., Rossum-Fikkert, S. E., van Elk, R., van Nierop, P., Smit, A. B., and Sixma, T. K. (2005) *J. Biol. Chem.* **280,** 26457–26466
44. Celie, P. H., Rossum-Fikkert, S. E., van Dijk, W. J., Brejc, K., Smit, A. B., and Sixma, T. K. (2004) *Neuron* **41,** 907–914
45. Ulens, C., Hogg, R. C., Celie, P. H., Bertrand, D., Tsetlin, V., Smit, A. B., and Sixma, T. K. (2006) *Proc. Natl. Acad. Sci. U. S. A.* **103,** 3615–3620
46. Hansen, S. B., Sulzenbacher, G., Huxford, T., Marchot, P., Taylor, P., and Bourne, Y. (2005) *EMBO J.* **24,** 3635–3646
47. Dewan, J. C., Grant, G. A., and Sacchettini, J. C. (1994) *Biochemistry* **33,** 13147–13154
48. Oswald, R. E., Sutcliffe, M. J., Bamberger, M., Loring, R. H., Braswell, E., and Dobson, C. M. (1991) *Biochemistry* **30,** 4901–4909
49. Moise, L., Piserchio, A., Basus, V. J., and Hawrot, E. (2002) *J. Biol. Chem.* **277,** 12406–12417
50. Harel, M., Kasher, R., Nicolas, A., Guss, J. M., Balass, M., Fridkin, M., Smit, A. B., Brejc, K., Sixma, T. K., Katchalski-Katzir, E., Sussman, J. L., and Fuchs, S. (2001) *Neuron* **32,** 265–275
51. Samson, A., Scherf, T., Eisenstein, M., Chill, J., and Anglister, J. (2002) *Neuron* **35,** 319–332
52. Zeng, H., Moise, L., Grant, M. A., and Hawrot, E. (2001) *J. Biol. Chem.* **276,** 22930–22940
53. Johnson, D. A. (2005) *Biophys. Chem.* **116,** 213–218
54. Hogg, R. C., Miranda, L. P., Craik, D. J., Lewis, R. J., Alewood, P. F., and Adams, D. J. (1999) *J. Biol. Chem.* **274,** 36559–36564